

TOWARDS LOW COST, EFFICIENT AND STABLE ORGANIC PHOTOVOLTAIC MODULES

Ronn Andriessen¹, Yulia Galagan¹, Jan-Eric Rubingh¹, Nadia Grossiord¹, Paul Blom¹, Jan Kroon², Sjoerd Veenstra², Wiljam Verhees², Lenneke Slooff², Paul Pex²

¹ Holst Centre, PO BOX 8550, 5605 KN Eindhoven, The Netherlands

² Energieonderzoek Centrum Nederland (ECN) Postbus 1, 1755 ZG Petten, The Netherlands

ABSTRACT: The presence of a transparent conductive electrode such as indium tin oxide (ITO) limits the reliability and cost price of organic photovoltaic devices as it is brittle and expensive. Moreover, the relative high sheet resistance of an ITO electrode on flexible substrates limits the maximum width of a single cell. Holst Centre and ECN have developed an alternative ITO-free transparent anode, based on a solution processed high conductive and transparent PEDOT:PSS layer in combination with a printed current collecting grid. Screen printed silver grids can yield sheet resistances down to 1 Ohm/Sq with a surface coverage of only ca 5%. The efficiency of a flexible device with an active area of 4 cm² with such a grid is much higher than a similar device based on ITO. Furthermore, as this composite anode is solution-processed, it is an important step forward towards low-cost large area processing. Moreover, initial experiments indicate that the stability of ITO-free devices is higher than the stability of standard devices based on ITO. This work will ultimately contribute toward fully printed devices, which will provide low-cost manufacturing and improved stability of organic photovoltaic modules.

Keywords: Organic solar cells, Current collecting grid, Lifetime

1 INTRODUCTION

The strongest motivation for the development of organic photovoltaic (OPV) cell technology is the low cost potential, based on the use of low-cost materials and substrates and the very high production speeds that can be reached by using roll-to-roll printing and coating techniques[1–6]. However, indium tin oxide (ITO), which is commonly used as transparent electrode, is one of the main cost consuming elements in present OPV devices, due to its material cost (In), the necessity of vacuum deposition and annealing and its multi-step patterning [1, 7]. A second argument to omit ITO from OPV devices is mechanical flexibility. The brittle ITO layer can be easily cracked, leading to a decrease in conductivity and as a result degradation of the device performance. This of course conflicts with the idea of having flexible and bendable OPV cells. A third argument for avoiding ITO is the presence of inhomogeneities of ITO when deposited on plastic substrates. These can be spikes due to the moderated annealing temperatures dictated by the glass transition temperature of the flexible substrates used (PET, PEN, ...). These spikes in turn can cause shorts in the devices as the subsequent layer thicknesses are often much thinner than the spikes present. Due to the limitations in annealing temperature of ITO on flexible plastic substrates, also in homogeneities in the conductivity are often present. These can cause severe limitations in the final module efficiency as the regions of the lowest conductivity will ultimately determine cell and module efficiency. A forth argument to omit ITO in OPV applications is the limited conductivity of it when deposited on plastic foils. With typical sheet resistances of 40 – 80 Ohm/Sq, it only allows individual cell widths of 6 to 10 mm. Widening cells will have an immediately negative effect on efficiency.

A lot of effort has been directed on the development of highly conductive polymeric materials such as poly(3,4-ethylenedioxy-thiophene):poly(4-styrenesulphonate) (PEDOT:PSS). Replacement of ITO by highly conductive PEDOT:PSS has been intensively

investigated and reported [8–12]. Although recent material improvements in the PEDOT:PSS composition resulted in conductivities up to 500 S.m⁻¹, it is still a factor 2 to 4 lower compared to ITO deposited on plastic substrates. Improving the conductivity of such a polymeric electrode is possible by combining it with a metal grid, which is either thermally evaporated through micro structured shadow masks [13, 14] or patterned by a lithographic method [15, 16]. In Ref. [17] deposition of an Ag grid by the photographic process of diffusion transfer reversal has been reported. Printing of the metal grid, however, is a prerequisite for fully printed OPV devices, enabling low-cost manufacturing. Recent newly developed silver nano-particle based inks (e.g. Suntronic, Sun Chemicals) and/or silver complexes based inks (e.g. Inktec) allow for sintering temperatures below 120 °C, which is compatible with plastic substrates as PET or PEN. These inks can yield resistivity values down to 3 times the value of bulk silver. Of course, these grid structures could also be combined with ITO to create larger efficient cell sizes. Apart from some specific interaction issues observed, this option will not bring solutions for the three first arguments against using ITO as summarized before.

Screen printed silver grids [4] were demonstrated in a roll-to-roll processed inverted OPV device, where the grid is the last printed layer in the devices. Earlier, we have reported inkjet printed current collecting grids as a part of a composite anode in a conventional OPV device [18], where the grid is the first printed layer in the devices. Integration of a conductive grid significantly decreases the resistance of the polymer anode. Despite the fact that single pass inkjet printed current collection grids demonstrate a sheet resistance of 15 Ohm/Sq with printed area coverage of about 10%. As this is still a high value for large area devices, it is anyhow better than what can be reached with ITO on a flexible substrate.

The conductivity of the grid can be improved by increasing the line height, but the increase in topology of the grid hinders the over coating of it with the subsequent thin layers. In this paper we report on OPV devices based on a current collecting grid. The metal grid has a sheet

resistance of 1 Ohm/Sq with surface area coverage lower than 10% and is free from any topology issues.

2 EXPERIMENTAL

A series of organic solar cell devices were prepared on glass and flexible PEN substrates. The layouts of the ITO-based and ITO-free devices are shown in Figure 1.

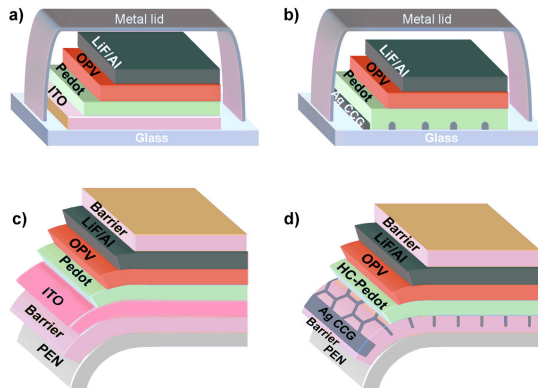


Figure 1: Schematic illustration of an ITO-based device and a device with a current collecting grid.

ITO sputtered on glass shows a sheet resistance of 15 Ohm/Sq. ITO sputtered on barrier coated PEN substrates shows a sheet resistance of 60 Ohm/Sq. ITO was patterned by using photo lithography. As a substrate, 125 μm thick thermally stabilized PEN from DuPont-Teijin Films was used [19]. The barrier layer was coated using Holst Centre thin film barrier technology [20]. The current collecting grids were deposited by screen and inkjet printing. Screen printing was performed using a DEK Horizon 03i screen printer with a SD 40/25 400 mesh screen. As material Inktec TEC-PA-010 hybrid nano silver paste with a silver content of 55 ± 10 wt% was used. This silver paste is a blend of silver nano particles and a soluble silver complex. Cabot AG-IJ-G-100-S1 silver nano particle ink has been used for the inkjet printing of the conductive grids. Immediately after printing the substrates are placed in a temperature controlled oven for 30 minutes at 135°C. The resulting current collecting grid lines are visually inspected with a microscope, followed by measuring the sheet resistance (Keithley 2400 Source Meter) and cross section area (Veeco Dektak Profilometer) of the lines on 5 different places of the grid. For the inkjet experiments a FujiFilm Dimatix Materials Printer (DMP 2831) with 10 pl drop size print heads is used. The drop spacing was set to 30 μm , while the chuck temperature was fixed at 20°C.

Low conductive PEDOT:PSS (Clevios PVPAI4083 PEDOT:PSS from H.C. Starck) was used for the preparation of the ITO-based devices. The PEDOT:PSS was spin coated at 2000 rpm, resulting in a dry layer thickness of 40 nm on top of the ITO layer after baking at 150°C for 10 min.

For the devices free from ITO, the highly conductive Orgacon™ PEDOT:PSS from Agfa-Gevaert was used. This highly conductive PEDOT:PSS was spin coated at 800 rpm, resulting in a dry layer thickness of 100 nm.

Poly-3-hexylthiophene, (P3HT, purchased from Plextronics, Plexcore OS2100) and [6,6]-phenyl-C61-

butyric acid methyl ester (PCBM) (99%, purchased from Solenne BV) were dissolved in 1,2-dichlorobenzene with a mixing ratio of 1:1 by weight. The solution was stirred for 14h at 70°C. The photoactive layers were obtained by spin coating of the blend with 4 wt% of the active materials at 1000 rpm for 30s, which results in a dry layer thickness of 220 nm.

The thicknesses of the films were measured using a Dektak profilometer. The experiments are performed in a clean room environment at ambient atmosphere. The metal cathode (1nm LiF, 100nm Al) was thermally evaporated in a vacuum chamber through a shadow mask. The OPV devices were finished by thin film encapsulation in a glove box. The active area of the devices was $2 \times 2 \text{ cm}^2$.

Current-voltage curves were measured using simulated AM1.5 global solar irradiation (100mW/cm^2), using a xenon-lamp-based solar simulator Oriel (LS0104) 150W. The light source was calibrated with a standard Si photodiode detector. UV-vis transmission/absorption spectra were measured using a Perkin-Elmer Lambda 12 UV/vis spectrophotometer.

3 RESULTS AND DISCUSSION

Figure 2(a) shows a picture of a typical part of a screen printed honeycomb current collecting grid, which is part of the composite anode. The corresponding line profile as shown in Figure 2(b) is relatively smooth. The effective line width was 160 μm width a peak height of 2 to 2.3 μm and the sheet resistance of the screen printed grid was 1 Ohm/Sq with an area coverage of 6.4% which is in a very good agreement with the theoretically expected values.

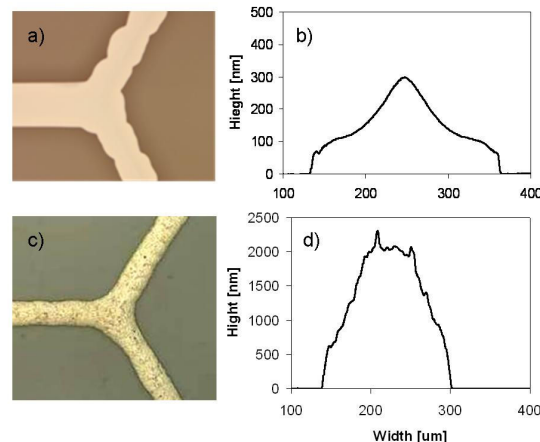


Figure 2: a) 50x optical microscope image and b) typical line profile of inkjet printed silver lines (grid) on barrier coated PEN film; c) 50x microscope image and d) a typical line profile of screen printed Inktec TEC-PA-010 ink.

The spreading behavior of the ink with inkjet printing depends on the surface energy of the substrate. As the surface energy of the used upper layer of the barrier stack (SiN) is relatively high, the resulting lines are much wider than the set value of 100 μm . To get the same surface properties for both the glass and foil substrates, we used glass substrates with a pre-coated thin SiN layer. The effective line width of the inkjet printed silver grids is about 180 μm with a maximum peak height of 300 nm.

The sheet resistance of the printed grid is 10 Ohm/Sq with an area coverage of 7.2 % which is in a very good agreement with the theoretically expected values. A microscopic image and a typical line profile are shown in Figure 2 (c,d).

The over-coatability over the inkjet-printed current collecting grid is tested by spin coating of PEDOT:PSS, followed by optical inspection. Prior to over-coating the substrates were treated with nitrogen plasma in order to level the surface energies of the SiN and the printed silver areas. As the profile of the conductive lines is very smooth and the height is relatively low, the spin coated PEDOT:PSS layer showed no visual defects.

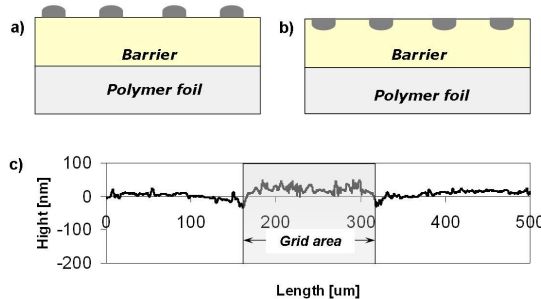


Figure 3: Schematic illustration of current collection grids: a) printed on top and b) embedded into the barrier. c) Dektak profile of the surface with embedded grid.

Overcoating of the screen printed grid with PEDOT:PSS using spin coating was not successful due to the height of the lines: 2 μm height seems to be much to high. This problem could be solved by embedding the grid in the barrier stack as schematically shown in Figure 3. As the procedure of embedding is part of the intellectual property of Holst Centre, no details can be revealed at this stage. Anyway, by embedding the conductive grid in the barrier stack a perfectly smooth surface containing the current collecting grid was obtained (see Figure 3(c)).

Honeycomb structures are often applied when the pattern should be less perceptible for the human eye, as is the case for e.g. Organic Light Emitting Diode (OLED) for lighting applications. As for OLED devices, the current is “injected” in the device area, the cross-points of the honeycomb grid ensure an homogeneous charge distribution in case of a point defect in the conductive grid pattern. This is not so when using line patterns. For (O)PV applications, line patterns can be safely used in as the charges are collected in the grid. In this case, a point defect in the conductive grid will only have a minor effect of the charge collection efficiency, as the charges can still run through the transparent conductive electrode at short distances.

In this short study, embedded conductive line patterns were compared with embedded conductive honeycomb structures. For the honeycomb pattern a pitch size of 5 mm is used, which results with an actual line width of 160 μm in an area coverage of 6.4%. For the line pattern, by using a pitch size of 2 mm, this resulted in an area coverage of 8%. The honeycomb pattern has a sheet resistance of 1 Ohm/Sq, whereas the line pattern has a sheet resistance of 0.8 Ohm/Sq.

Table I: Characteristics of photovoltaic devices on glass substrates

Anode	Jsc [mA/cm ²]	Voc [Volt]	FF [%]	η [%]
ITO (15 Ohm/Sq)	7.51	0.526	52.3	2.07
HC-PEDOT (350 Ohm/Sq)	4.93	0.534	32.7	0.86
Inkjet pr. Ag (10 Ohm/Sq) / HC-PEDOT	5.30	0.537	53.4	1.52

Table II: Characteristics of the photovoltaic devices on flexible PEN/Barrier substrates

Anode	Jsc [mA/cm ²]	Voc [Volt]	FF [%]	η [%]
ITO (60 Ohm/Sq)	6.59	0.489	29.6	0.95
Scr. Pr. & embedded Ag honeycombs (1 Ohm/Sq) / HC-PEDOT	6.36	0.540	53.0	1.82
Scr. Pr. & embedded Ag lines (0.8 Ohm/Sq) / HC-PEDOT	6.25	0.540	57.1	1.93

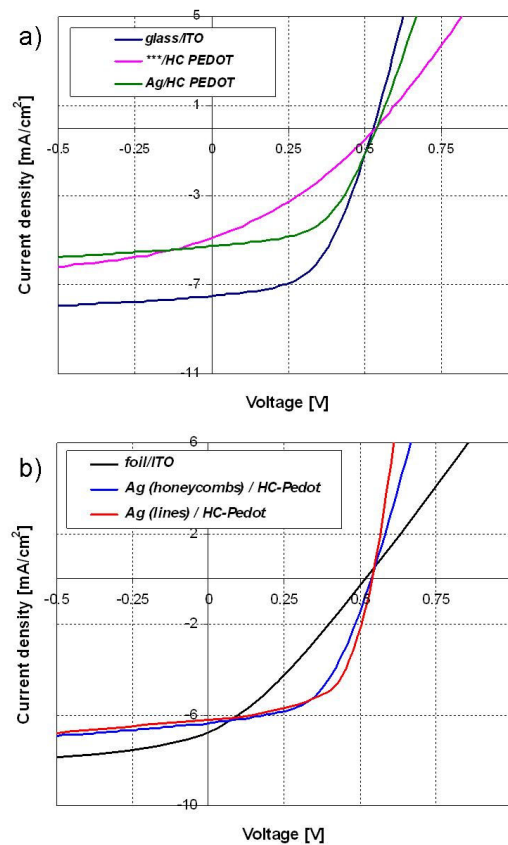


Figure 4: a) JV-curves of OPV devices with an active area of 2x2 cm² on glass substrate with different anodes: ITO (dark blue), high conductive PEDOT:PSS (pink) and high conductive PEDOT:PSS with metal grid (green), b) JV-curves of flexible OPV devices with an active area of 2x2 cm² with different anodes: ITO (black), high conductive PEDOT:PSS with respectively a honeycomb (blue) and a line (red) pattern current collecting grid.

The characteristics of an ITO-based solar cells and the solar cells with composite anode (current collecting grids and high conductive PEDOT:PSS) are given in Table I for the devices on glass substrates and in Table II for the flexible devices on PEN/barrier foil. The current-voltage curves are shown in Figure 4.

By comparing the results of the ITO containing devices on glass (Table I and Figure 4a) with the results of the ITO containing devices on PEN foil, (Table II and Figure 4b), the negative effect on the cell performance (mainly a decrease in fill factor) by increasing the sheet resistance from 15 Ohm/Sq (ITO on glass) to 60 Ohm/Sq (ITO on foil) becomes immediately clear for these devices with dimensions of $2 \times 2 \text{ cm}^2$. Replacing ITO on glass by highly conductive PEDOT is not an option as is shown in Table I and Figure 4a because the sheet resistance is even lower compared to ITO on foil. Including a conducting grid (in this case inkjet printed silver which results in a sheet resistance of ca 10 Ohm/Sq) improves dramatically the fill factor. The reason for the lower J_{sc} is not yet fully clear, but could be caused by non-optimal layer thickness settings (cfr. later).

Theoretical calculations [21] show that scaling up the size of solar cell devices on plastic foils using ITO as transparent electrode is not possible without efficiency losses due to a substantial decrease in fill factor which is related to the resistance of the ITO. The optimal cell width for ITO-based devices on a plastic substrates is in the range of 0.5–1.0 cm. The $2 \times 2 \text{ cm}^2$ ITO-based device yields a fill factor of 29.6% and an efficiency of 0.95%. Again, replacing ITO on foil by only a high conductive PEDOT:PSS (HC-PEDOT) leads to a further decrease of the short-circuit current [18]. This is caused by the even higher sheet resistance of the HC-PEDOT, which is in the range of 200–500 Ohm/Sq, depending on the exact transparency values (typically between 85 and 90%). Therefore, it is very important to increase the conductivity of the anode in order to be able to produce cells with significant dimensions which in turn will only help in increasing the active area of the final modules. This is possible by adding the current collecting grid. The benefits are clearly illustrated in Table II and figure 4b, were a substantial performance increase can be observed when replacing the ITO on foil by the composite electrode consisting of highly conductive PEDOT and printed and embedded metal conductive grids. The difference in current density for devices with such grids versus ITO-based devices can be partly explained by differences in shadow losses due to the grids. Thus, the value of J_{sc} for the device with the honey comb grid is somewhat higher than that for the device with the line grid. With the honeycomb pattern, 6.4% of the surface is covered by the grid, while the line pattern covers 8% of the surface. This explains the small but observed difference in the J_{sc} between the two grid-based devices.

Apart from the shadow losses by the grid, the transparency difference between the double layer ITO/low conductive PEDOT and the highly conductive PEDOT needs to be taken into account. The 120 nm layer of ITO on PEN provides an average transmittance of 90% over the visible spectrum (400–700 nm). The subsequent 40 nm layer of low conductive PEDOT also absorbs a part of the solar spectrum. The question now is whether this double layer yields lower or higher transparency compared to the 100 nm thick layer of highly conductive PEDOT. The summarized transmission spectra of the

stacks PEN/barrier/ITO /40nm LC-PEDOT and PEN/barrier/100nm HC-PEDOT are shown in Figure 5.

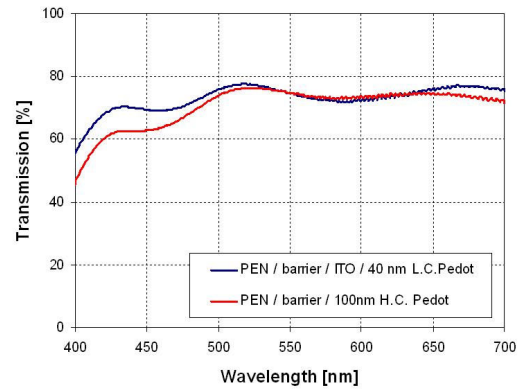


Figure 5: Transmittance of the device stacks: PEN/barrier/ITO with 40 nm LC-PEDOT:PSS versus PEN/barrier/ with 100 nm HC-PEDOT:PSS.

The transmission spectra indicate that transmittance of light into the photo active layer is higher in the case of the ITO-based device. The 100 nm thick layer of high conductive PEDOT has a relatively high absorption in the visible region. This fact can partly explain the difference in measured current in both types of devices. Moreover, interference effects should be taking into account. The thickness of the active layer (± 220 nm), according to optical modeling [22, 23], was optimal for the ITO-based devices with a 40 nm thick PEDOT layer. Such ratio in the layer thicknesses seems to provide a maximum value for J_{sc} . Omitting ITO and replacement of low conductive PEDOT by highly conductive PEDOT with a different layer thickness can result in extra negative interferences in the layer stacking, which in turn can negatively affect J_{sc} . Most probably, the optimum layer thickness of the photo-active layer will be different from the 220 nm used on top of an ITO/low conductive PEDOT stack. Additional modeling will be needed to assist the identification of a proper layer stack setting. Additionally, as already mentioned above, the shadow effect of the grids contributes to the lower current density in the ITO-free devices. The sum of all these factors explains why the current density in ITO-based and ITO-free devices is different. Further improvement of the current density in ITO-free devices is possible by decreasing the shadow effect, by minimizing the line width in the grids and by increasing the transparency of the high conductive PEDOT and optimization of layer thicknesses.

The solar cells with the composite anode versus ITO-based devices show almost the same open-circuit voltage (V_{oc}) values, but the fill factors significantly differ. Introduction of a conductive grid with a sheet resistance of $1 \Omega/\square$ into the photovoltaic devices substantially improves the fill factor. As the HC-PEDOT is still responsible for the current collection in the area between the grid lines, the high conductivity of this PEDOT is very important. Moreover, the distance between the grid lines is an important parameter for successful current collection. In [14] the optimum pitch size has been calculated in wrap-through OPV devices for PEDOTs with different conductivities. In this paper two different pitch sizes have been tested. The results illustrate that the

device with the line pattern, with a pitch size of 2 mm, has a higher fill factor than the honeycomb pattern, which has a pitch size of 5 mm.

As the data show, replacing the ITO by a composite anode, consisting of combination of a metal grid and HC-PEDOT, results in a significant increase in efficiency for devices of $2 \times 2 \text{ cm}^2$. Future work will concentrate in maximizing the cell area without substantial efficiency losses by using optimized grid structures. This will enable a substantial increase of the active area of OPV modules which in turn will increase the final Wp/m^2 .

The life time of the devices is determined by both intrinsic and extrinsic stabilities. The influence of the external factors like water, oxygen, (UV) light and combinations thereof determine the extrinsic stability of the OPV devices. Without decent encapsulation, the life time of the devices reported in this study is limited to a few hours, due to the highly reactive cathode used in this case (Aluminium). A high quality barrier can significantly extend the life time of the devices. However, well protected devices from external factors can still lose their properties due to intrinsic interactions between the layers. A study of the intrinsic stability of the ITO-free devices and a comparison with the intrinsic stability of "standard" ITO-based devices has been performed on devices with the following layouts:

- glass/ITO/PEDOT/P3HT:PCBM/LiF/Al
- glass/ HC-PEDOT/P3HT:PCBM/LiF/Al.
- glass/Ag-grid/HC-PEDOT/P3HT:PCBM/LiF/Al

The above listed devices were all prepared on glass substrates, as glass provides good barrier properties from one side of the devices. The other side of the devices was protected by a stainless steel lid which was hermetically sealed by using epoxy glue. Identical sets of devices have been tested under three different conditions: in the dark at room temperature, in the dark at a temperature of 45°C and illuminated (1,5AM condition) at 45°C . The cells, which were kept in the dark at room temperature, remained stable over time. At an elevated temperature in the dark, the efficiency of ITO-based devices drops. The efficiency of the ITO-free devices, both with and without Ag grid, did not change. The combination of light and elevated temperature shows a very rapid degradation of the ITO-based devices. At the same time the efficiency of the ITO-free devices remains almost unchanged. The relative changes of the efficiency of the devices stored at 45°C under the light are given in Figure 6.

Light and temperature are the two main factors which speed up the degradation of the solar cells. In the described experiment we have used encapsulated devices. The quality of the sealant is such that leakage of water and oxygen from the environment does not play a significant role during the test period. All observed changes in the device performance are related to the intrinsic stability of the devices. It is clear that devices containing ITO degrade much faster than ITO-free devices. This fast degradation of ITO-based devices is explained by the indium diffusion through all layers in such devices [24, 25]. Indium migration results in conductivity losses in the ITO anode. These conductivity losses lead to an increase of the series resistances in the devices and as a result the fill factor drops down.

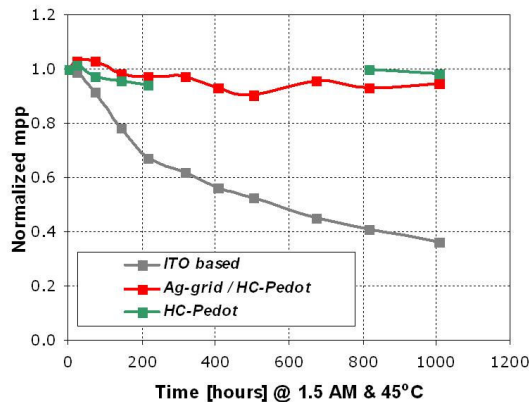


Figure 6: Relative changes of the efficiency over the time, stored at 45°C with light exposure for the devices on glass substrate with different anodes: ITO (gray), high conductive PEDOT (green) and high conductive PEDOT with metal grid (red).

For non-flexible applications of OPV's the use of glass and metal lids in combination with encapsulated getter materials is a good and reliable method. However, flexible devices require a thin film encapsulation that will allow roll-to-roll manufacturing of organic photovoltaics. Thin film barrier technology of Holst Centre has been compared with metal lid encapsulation. For that, identical ITO-based devices were prepared on glass substrate and encapsulated either with metal lid or with thin film barrier of Holst Centre. As ITO-based devices have been chosen as tested devices, which are not stable due to intrinsic factors, they degrade over time. However, the observed performance losses by using thin film encapsulation are similar as for metal lid encapsulated devices (see Figure 7). This indicates that the thin film barrier developed at Holst Centre is basically as good for organic photovoltaics as the metal lid encapsulation.

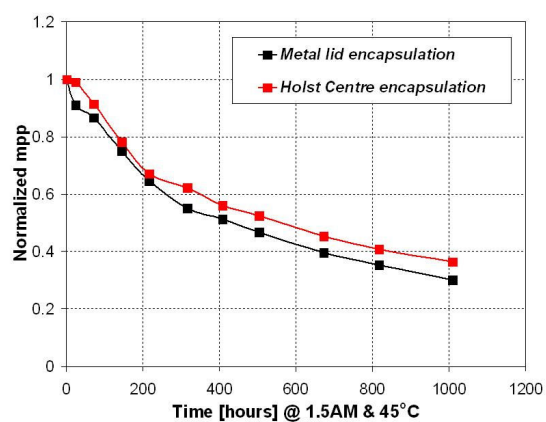


Figure 7: Relative changes of the efficiency over the time, stored at 45°C with light exposure for the ITO-based devices on glass substrate with metal lid encapsulation (black) and Holst Centre encapsulation (red).

4 CONCLUSIONS

Organic solar cells free from ITO on flexible substrates were fabricated. The alternative anode is based

on highly conductive PEDOT:PSS in combination with printed current collecting grids. This type of composite anode has a significantly lower sheet resistance in comparison with ITO, which makes larger area devices possible without substantial efficiency losses. The experiments show that the replacement of ITO on foil by a composite anode yields an efficiency increase by a factor of two for devices with an active area of $2 \times 2 \text{ cm}^2$. Moreover, the intrinsic stability of ITO-free devices is much higher than the stability of devices based on ITO. After 1000 hours at elevated temperature and light exposure, the encapsulated ITO-free devices keep their initial performance. Whereas the devices with an ITO electrode show more than 60% of efficiency loss at these conditions. Additionally, the anode is entirely fabricated using solution processing techniques and does not require high temperature annealing nor litho steps. All temperature treatments are compatible with flexible substrates and roll-to-roll processing. Free from the rather expensive vacuum deposited ITO, the composite electrode can significantly decrease manufacturing cost. This work will ultimately contribute towards fully printed devices, which will provide low-cost roll-to-roll manufacturing.

5 ACKNOWLEDGEMENTS

This work has been supported in part by the European Commission as part of the Framework 7 ICT 2009 collaborative project HIFLEX (Grant agreement no.248678) and by the Dutch ministry of economic affairs of the Netherlands.

6 REFERENCES

- [1] F.C. Krebs, Roll-to-roll fabrication of monolithic large-area polymer solar cells free from indium-tin-oxide, *Sol. Energy Mater. Sol. Cells* 93 (2009) 1636-1641.
- [2] Y. Galagan, I. de Vries, A. Langen, R. Andriessen, W. Verhees, S. Veenstra, J. Kroon, Technology development for roll-to-roll production of organic photovoltaics, *Chem. Eng. Process.* (2010) doi:10.1016/j.cep.2010.07.012.
- [3] F.C. Krebs, Fabrication and processing of polymer solar cells: A review of printing and coating techniques, *Sol. Energy Mater. Sol. Cells* 93 (2009) 394-412.
- [4] F.C. Krebs, Polymer solar cell modules prepared using roll-to-roll methods: Knife-over-edge coating, slot-die coating and screen printing, *Sol. Energy Mater. Sol. Cells* 93 (2009) 465-475.
- [5] L. Blankenburg, K. Schultheis, H. Schache, S. Sensfuss, and M. Schrödner, Reel-to-reel wet coating as an efficient up-scaling technique for the production of bulk-heterojunction polymer solar cells, *Sol. Energy Mater. Sol. Cells* 93 (2009) 476-483.
- [6] A.J. Medford, M.R. Lilliedal, M. Jørgensen, D. Aarø, H. Pakalski, J. Fyenbo, and F.C. Krebs, Grid-connected polymer solar panels: initial considerations of cost, lifetime, and practicality, *Opt Express* 18 (2010) A272-A285.
- [7] F.C. Krebs, T. Tromholt, and M. Jorgensen, Upscaling of polymer solar cell fabrication using full roll-to-roll processing, *Nanoscale* 2 (2010) 873-886.
- [8] Y. Zhou, F. Li, S. Barrau, W. Tian, O. Inganäs, and F. Zhang, Inverted and transparent polymer solar cells prepared with vacuum-free processing, *Sol. Energy Mater. Sol. Cells* 93 (2009), 497-500.
- [9] S.K. Hau, H.-L. Yip, J. Zou, and A.K.Y. Jen, Indium tin oxide-free semi-transparent inverted polymer solar cells using conducting polymer as both bottom and top electrodes, *Organ. Electron.* 10 (2009) 1401-1407.
- [10] B. Winther-Jensen and F.C. Krebs, High-conductivity large-area semi-transparent electrodes for polymer photovoltaics by silk screen printing and vapour-phase deposition, *Sol. Energy Mater. Sol. Cells* 90 (2006) 123-132.
- [11] E. Ahlsweide, W. Muhleisen, M.W.b.M. Wah, J. Hanisch, and M. Powalla, Highly efficient organic solar cells with printable low-cost transparent contacts, *Appl. Phys. Lett.* 92 (2008), 143307.
- [12] Y.-M. Chang, L. Wang, and W.-F. Su, Polymer solar cells with poly(3,4-ethylenedioxythiophene) as transparent anode, *Organ. Electron.* 9 (2008) 968-973.
- [13] M. Glatthaar, M. Niggemann, B. Zimmermann, P. Lewer, M. Riede, A. Hinsch, and J. Luther, Organic solar cells using inverted layer sequence, *Thin Solid Films* 491 (2005), 298-300.
- [14] B. Zimmermann, M. Glatthaar, M. Niggemann, M.K. Riede, A. Hinsch, and A. Gombert, ITO-free wrap through organic solar cells-A module concept for cost-efficient reel-to-reel production, *Sol. Energy Mater. Sol. Cells* 91 (2007) 374-378.
- [15] K. Tvingstedt and O. Inganäs, Electrode Grids for ITO Free Organic Photovoltaic Devices, *Adv. Mater.* 19 (2007), 2893-2897.
- [16] J. Zou, H.-L. Yip, S.K. Hau, and A.K.Y. Jen, Metal grid/conducting polymer hybrid transparent electrode for inverted polymer solar cells, *Appl. Phys. Lett.* 96 (2010) 203301-203303.
- [17] T. Aernouts, P. Vanlaeke, W. Geens, J. Poortmans, P. Heremans, S. Borghs, R. Mertens, R. Andriessen and L. Leenders, Printable anodes for flexible organic solar cell modules, *Thin Solid Films* 451-452 (2004), 22-25.
- [18] Y. Galagan, R. Andriessen, E. Rubingh, N. Grossiord, P. Blom, S. Veenstra, W. Verhees, and J. Kroon, Toward fully printed Organic Photovoltaics: Processing and Stability, *Lope-C* (2010) 88-91.
- [19] I. Yakimets, D. MacKerron, P. Giesen, K.J. Kilmartin, M. Goorhuis, E. Meinders, and W.A. MacDonald, Polymer substrates for flexible electronics: Achievements and challenges, *Adv. Mat. Res.* 93-94 (2010) 5-8.
- [20] F. v. Assche, H. Rooms, E. Young, J. Michels, T. v. Mol, G. Rietjens, P. v. d. Weijer, and P. Bouting, Thin-film barrier on foil for organic LED lamps, AIMCAL Fall Technical Conference and 22nd International Vacuum Web Coating Conference (2008).
- [21] C. Lungenschmied, G. Dennler, H. Neugebauer, S.N. Sariciftci, M. Glatthaar, T. Meyer, A. Meyer, Flexible, long-lived, large-area, organic solar cells, *Sol. Energy Mater. Sol. Cells* 91 (2007) 379-384.
- [22] A.J. Moule, J.B. Bonekamp, K. Meerholz, The effect of active layer thickness and composition on the performance of bulk-heterojunction solar cells, *J. Appl. Phys.* 100 (2006) 094503-094507.

- [23] A.J. Moulé, K. Meerholz, Minimizing optical losses in bulk heterojunction polymer solar cells, *Appl. Phys. B* 86 (2007) 721-727.
- [24] M. Jørgensen, K. Norrman, F. C. Krebs, *Sol. Energy Mater. Sol. Cells* 92 (2008) 686-714.
- [25] F. C. Krebs, K. Norrman, *Prog. Photovoltaics* 15 (2007) 697-712.